Bubble Formation in Additive Manufacturing of Borosilicate Glass

Junjie Luo*, Theresa Bender*, Douglas A. Bristow*, Robert G. Landers*, Jonathan T. Goldstein†, Augustine M. Urbas† and Edward C. Kinzel*
*Mechanical and Aerospace Engineering, Missouri University of Science and Technology, 400 W. 13th St., Rolla, MO, USA 65409;
†Air Force Research Laboratory, Materials and Manufacturing Directorate, Wright-Patterson Air-Force Base, OH, USA 45433

Abstract

Entrapped bubbles are an important problem in conventional glass manufacturing. It is also a significant factor determining the quality of glass products produced using additive manufacturing (AM). This paper reports on the bubble formation and entrapment in filament-fed AM printing of borosilicate glass. This process involves maintaining a local molten region using a CO_2 laser. A 2 mm filament is fed continuously into the molten region while CNC stages position the workpiece relative to the laser and filament feed. Two different bubble regimes are identified in experiments with borosilicate glass. These regimes can be related to different physical phenomena, specifically, bubble entrapment at defects in the filaments and bubble formation due to reboil. These can be overcome by selecting defect free filaments and by minimizing the temperature inside the molten region to prevent breaking down the glass. Understanding these mechanisms allows bubble-free glass to be printed. Finally, residual stress in the deposited glass pieces is removed using post-deposition annealing and validated using a polariscope.

Introduction

Additive manufacturing has been widely studied for structural parts using numerous materials, such as metals, polymers, and ceramics [1]. Several studies has considered AM of transparent optical elements. Most of these studies have focused on transparent polymer materials, including fused deposition modeling [2-4], ink-jet printing [5,6], selective laser melting (SLS) with post index matched resin infiltration [7], and multiphoton stereolithography [8]. Though these techniques are able to print transparent parts, their applications are limited since the poor material properties compared to glasses and other inorganic materials.

Glasses are widely used in high quality and high power optics due to higher transmissivity, lower coefficient of thermal expansion, and more stable refractive indices [9]. However, there is limited published research on AM transparent glasses. Conventional, AM techniques have been studied for glass printing, including selective laser melting/ sintering (SLM/SLS) [10-14], and extrusion techniques [15]. However, only non-transparent structural parts have been printed using these techniques. Recent studies have demonstrated the production of 2D and 3D solid structures using transparent soda lime glass and even quartz feedstock [14-20]. Compared to soda lime glass, borosilicate glasses have a lower Coefficient of Thermal Expansion (CTE) (1/3 of soda lime glass [9]). This leads to a higher thermal shock resistance that makes it a better material for applications ranging from optics to glassware. Two issues that confront additive manufacturing of glasses (including both soda lime and borosilicate) are bubble entrapment/formation [20] and residual stresses due to rapid cooling of the glass during printing.

Bubble formation and entrapment is a significant issue for conventional glass industry. Bubbles cause optical scatter in glass which limits the optical performance. For example, six bubbles per ton of glass leads to a 10% rejection rate in television panel industry [21]. In addition to optical considerations, bubbles significantly weaken the glass mechanically. There are multiple sources of bubbles in conventional glass manufacturing, including air trapping, decomposition of the individual components that make up glass, galvanic oxidation reduction reactions, and “reboil”, which is the precipitation of super saturated glass when heated to a high temperature [22]. In our previous study of bubble formation in soda lime glass, three different forms of bubbles

were identified in printed soda lime glass; periodic bubbles, sporadic bubbles and foam layers [20]. The foam layers were likely a result of reboil due to over heating the glass with the laser, while the periodic and sporadic bubbles could be attributed to bubble entrapment at the lower interface of the printed track and bubble generation around defects or contamination in the filament, respectively.

In this paper, bubble formation in additive manufactured borosilicate glass is investigated. Two types of bubbles are identified for this glass system; filament defect/interface and reboil/volumetric defects. The physical phenomena associated with the two classes of bubbles are studied empirically. This helps understand the effects of the process parameters and leads to bubble-free borosilicate glass pieces. Finally, residual thermal stresses generated during the printing process are observed using a polariscope. These are removed using a post deposition annealing step without modifying the printed topography.

Experimental Setup

The experimental setup for glass filament fed additive manufacturing process is shown in Fig. 1. A CO_2 laser beam is incident on the top surface of the printed part. A glass filament is continuously fed into the intersection of the workpiece and the laser beam. The laser heats this interface to create a molten region above the glass transition temperature. The wavelength of the CO_2 laser is 10.6 µm, which directly couples to phonon modes in the glass. This leads to a very short optical penetration depth so that the laser is effectively a surface flux. The movement horizontal movement of the stage is realized by *x* and *y* stages (Aerotech ANT130-160XY), and a *z* stage (Aerotech ATS100-150) is used to raise and lower the platform. The filament is fed by a homebuilt feeder. 2 mm diameter borosilicate glass rods are used in this paper (McMaster Carr).

An unheated ceramic refractory block is used as the substrate. For small pieces of borosilicate glass printing, preheating of substrate to avoid thermal shock is not necessary because the CTE of borosilicate glass ($\sim 3\times10^{-6}$ K^{-1}) is only one third of that of soda lime glass. For larger printing larger pieces, the substrate may be needed to be heated to release the thermal stress. The laser is defocused to a Full Width Half Maximum (FWHM) diameter of 2 mm at build-plane filament intersection. A thermopile power meter (Ophir 10A–V1) is used to measure the reflected laser beam from the beam splitter, which is 1% of the laser energy delivered to the platform.

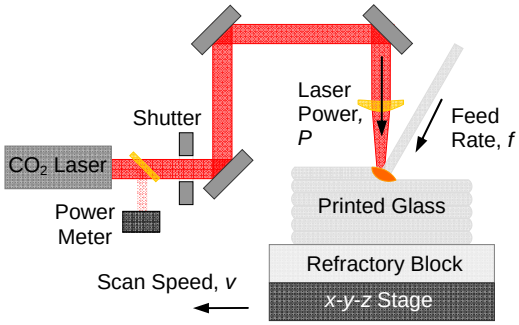

Fig. 1. Illustrate of filament fed glass AM setup

Results and Discussion

Figure 2 shows a dark field image of a printed piece of borosilicate glass. There are several clusters of bubbles visible in the specimen. Close observation reveals that the bubble clusters fall into two classes: (1) tightly spaced bubbles at the interfaces between tracks and (2) volumetrically distributed bubbles. Microscope images of the interface concentrated bubbles show that their typical diameter is on the order of 10 µm while the volumetric bubbles are less densely spaced and have bubble diameters ranging from 50 to 100 µm.

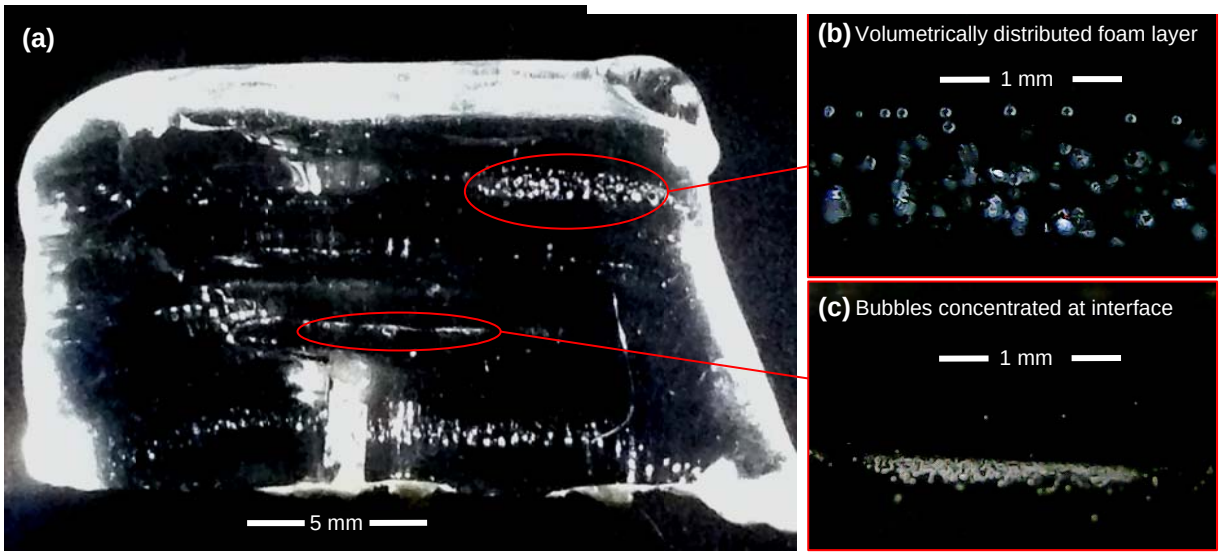

Fig. 2. An example of bubbles in a polished section of printed borosilicate glass (a) dark-field image of the whole wall (b) foam layer of volumetrically distributed bubbles (c) bubbles concentrated at interface.

Close inspection of the filaments revealed that many of them have scratches as received, prior to printing. These scratches are a possible source of bubble formation. To demonstrate this phenomenon, a diamond scribe was used to scratch a filament. The filament was laid on the x-y-z stage as opposed to feeding the filament into the molten region. The laser was scanned along the along the filament with a power of 25 W and a scan speed of 0.5 mm/s. Figure 3 shows dark field images of the results. After laser irradiation, the scratch disappears and is replaced by clusters of small bubbles with diameters on the range of 10 μm. This supports the hypothesis that surface defects on the filaments are the origin of the tightly clustered bubbles in Fig. 2(c) which appear at the interface between tracks and have a similar size distribution.

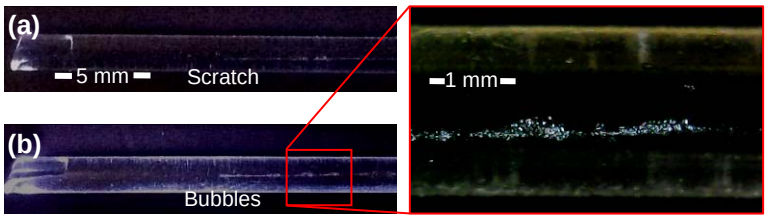

Fig. 3. Dark-field images of scratched filament (a) before and (b) after laser scanning

Selecting filaments without scratches avoids the type of bubbles in Fig. 3 and Fig 2(c). Single track wide walls were printed using a constant scan speed and feed rate, v=f=0.5 mm/s. After each row, the z-stage was lowered 1 mm. This was based off measurements of single track heights for the 2 mm diameter borosilicate filaments.

Six walls were printed Single walls could be printed from 25 to 50 W, while the filament could not be fully melted. All of the six walls are polished, and taken dark-field image to quantify the bubbles inside the samples. The bubble density of the walls is shown in Fig. 4. No bubbles were visible for low laser powers (≤30 W). At higher laser powers (≥35 W), foam layers could be observed. The average diameter of bubbles was larger at higher laser powers. Because of the removal of scratched filaments, no small bubbles at track interface were observed in any of the samples.

The temperature of molten region increases with laser power. The observation that the bubble concentration scales with laser power suggests that rate of bubble formation scales with temperature. The experimental results also show that below a laser power threshold the glass does not break down, which is consistent with the reboil phenomenon in conventional glass production. Vapor rising from the molten region

was observed for powers greater than 35 W which also supports a temperature driven chemical breakdown of the glass.

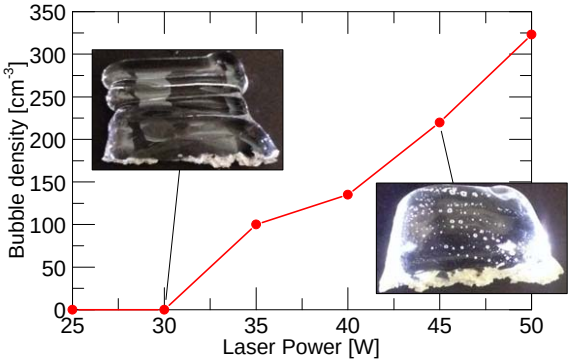

Fig. 4. Bubble density of the printed walls

Residual stresses are another important factor limiting the quality of printed glass. This issues is more significant for the borosilicate glass printed on an unheated platform than previous soda-lime work using a heated substrate. Beyond the risks of thermal shock, residual stresses are a significant issue for printed optics because they result in local index anisotropy [22] and reduced shatter resistance. While residual stresses are also a significant issue for many additive manufacturing processes, printing transparent glass offers a unique opportunity to study the phenomena. Stress induced birefringence can be detected using a polariscope [23].

Figure 5(a) shows an image through a polariscope of a single track sample as printed (prior to polishing). The bright regions indicate stress concentration. Future studies will explore the effects of path planning on the residual stress which is caused by uneven heating/cooling cycles during deposition. Annealing the sample can relieve trapped stresses. To demonstrate this, the sample in Fig. 5(a) was soaked in a 568°C in a muffle furnace for two hours before cooling to the strain point at 510°C over two hours and finally cooling to room temperature over the course of an hour. A polariscopic image of the sample after annealing is shown in Fig. 5(b). The stress-concentration is significantly reduced. It is important to see, that the morphology of the sample was not significantly affected by the annealing process.

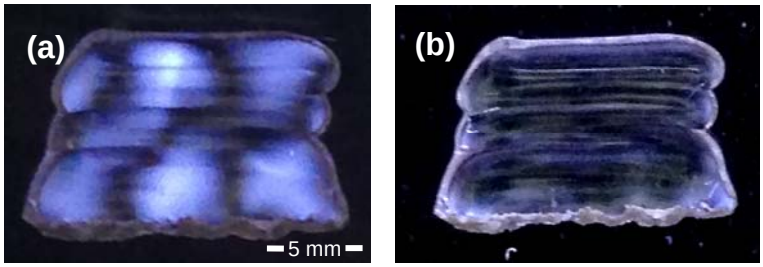

Fig. 5. Polariscope images of a printed borosilicate glass wall (a) before annealing (b) after annealing

The furnace annealed wall Fig 5(b) was then polished on both sides. The dark-field image of the polished wall is shown in Fig. 6. No bubbles are observed in the sample and the birefringence is clearly reduced.

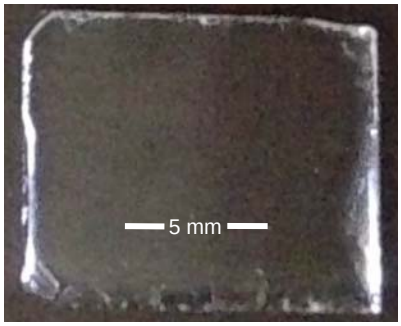

Fig. 6. Polariscope image of polished bubble-free glass wall after polishing

Summary and Conclusion

This paper explored additive manufacturing of borosilicate glass. Two different bubble regimes are identified in the printed borosilicate glass: small bubbles at track interface and foam layers. The formation small bubbles at track interface is traced to surface defects on the filament. The foam layers are traced to the reboil of glass at high temperatures. Bubble free glass can be produced by avoiding scratches on the filaments and minimizing the high temperature in the molten region by printing slower with lower laser power or using smaller diameter filaments. Significant residual stresses were observed in the printed pieces. These stresses were able to eliminated with a post annealing process without changing the overall morphology of the printed pieces. The elimination of bubbles and residual stress induced birefringence is key to printing glass for optical applications or low CTE structural elements.

Acknowledgment

This work was supported by the National Science Foundation (CMMI-1538464).

References

[1] Gibson, I., Rosen, D. W., and Stucker, B., 2010, *Additive Manufacturing Technologies*, Springer.
[2] Brockmeyer, E., Poupyrev, I., and Hudson, S., 2013, "PAPILLON: designing curved display surfaces with printed optics," Proc. ACM Symposium, St. Andrews, Scotland, pp. 457-462.
[3] Willis, K., Brockmeyer, E., Hudson, S., and Poupyrev, I., 2012, "Printed optics: 3D Printing of Embedded Optical Elements for Interactive Devices," Proc. ACM Symposium, Cambridge, MA, USA, pp. 589-598.
[4] Pereira, T., Rusinkiewicz, S., and Matusik, W., 2014, "Computational Light Routing: 3D Printed Optical Fibers for Sensing and Display," ACM Transactions on Graphics, 33(3), p. 24.
[5] Blessing, K., and Richard Van, d. V., 2014, "Print head, upgrade kit for a conventional inkjet printer, inkjet printer and method for printing optical structures," United States Patent Application: EP2661345 A1.
[6] Urness, A. C., Moore, E. D., Kamysiak, K. K., Cole, M. C., and McLeod, R. R., 2013, "Liquid deposition photolithography for submicrometer resolution three-dimensional index structuring with large throughput," Light: Science & Applications, 2(3), p. e56.
[7] Niino, T., and Yamada, H., 2009, "Fabrication of Transparent Parts by Laser Sintering Process:-Transparentization of Laser Sintered Plastic Parts by Infiltrating Thermosetting Epoxy with Tuned Refractive Index," Journal of the Japan Society for Precision Engineering, 75(12), pp. 1454-1458.
[8] Marder, S. R., Brédas, J.-L., and Perry, J. W., 2007, "Materials for multiphoton 3D microfabrication," MRS Bulletin, 32(07), pp. 561-565.
[9] Weber, M. J., 2002, *Handbook of Optical Materials*, CRC Press.
[10] Khmyrov, R., Grigoriev, S., Okunkova, A., and Gusarov, A., 2014, "On the Possibility of Selective Laser Melting of Quartz Glass," Physics Procedia, 56, pp. 345-356.
[11] Khmyrov, R. S., Protasov, C. E., Grigoriev, S. N., and Gusarov, A. V., 2015, "Crack-free selective laser melting of silica glass: single beads and monolayers on the substrate of the same material," International Journal of Advanced Manufacturing Technology, 85, pp. 1-9.
[12] Klocke, F., McClung, A., and Ader, C., 2004, "Direct Laser Sintering of Borosilicate Glass," Proceedings of the 15th SFF Symposium, Austin, TX, pp. 214-219.
[13] Fateri, M., and Gebhardt, A., 2015, "Selective Laser Melting of Soda-Lime Glass Powder," International Journal of Applied Ceramic Technology, 12(1), pp. 53-61.
[14] J. Luo, H. Pan, and E. C. Kinzel, 2014, "Additive Manufacturing of Glass," Journal of Manufacturing Science and Engineering, 136(6), pp. 061024-061024.
[15] Fu, Q., Saiz, E., and Tomsia, A. P., 2011, "Bioinspired Strong and Highly Porous Glass Scaffolds," Advanced Functional Materials, 21(6), pp. 1058-1063.
[16] Klein, J., Stern, M., Franchin, G., Kayser, M., Inamura, C., Dave, S., Weaver, J. C., Houk, P., Colombo, P., and Yang, M., 2015, "Additive Manufacturing of Optically Transparent Glass," 3D Printing and Additive Manufacturing, 2(3), pp. 92-105.

[17] Luo, J., Gilbert, L., Qu, C., Wilson, J., Bristow, D., Landers, R., and Kinzel, E., 2015, "Wire-Fed Additive Manufacturing of Transparent Glass Parts," Proc. International Manufacturing Science and Engineering Conference, Charlotte, NC.
[18] Luo, J., Gilbert, L., Qu, C., Morrow, B., Bristow, D., Landers, R., Goldstein, J., Urbas, A., and Kinzel, E., 2015, "Solid Freeform Fabrication of Transparent Fused Quartz Using a Filament-Fed Process," of the 26th SFF Symposium, Austin, TX, pp. 122-133.
[19] Luo, J., Gilbert, L. J., Bristow, D. A., Landers, R. G., Goldstein, J. T., Urbas, A. M., and Kinzel, E. C., "Additive manufacturing of glass for optical applications," Proc. SPIE Photonics West, San Francisco.
[20] Luo, J., Gilbert, L. J., Peters, D. C., Bristow, D. A., Landers, R. G., Goldstein, J. T., Urbas, A. M., and Kinzel, E. C., "Bubble formation in additive manufacturing of glass," Proc. SPIE Defense+ Security, pp. 982214-982216.
[21] Pilon, L., Fedorov, A. G., Ramkrishna, D., and Viskanta, R., 2004, "Bubble transport in three-dimensional laminar gravity-driven flow – mathematical formulation," Journal of Non-Crystalline Solids, 336(2), pp. 71-83.
[22] Shelby, J. E., 2005, *Introduction to Glass Science and Technology*, Royal Society of Chemistry.
[23] Aben, H., Ainola, L., and Anton, J., 2000, "Integrated photoelasticity for nondestructive residual stress measurement in glass," Optics and Lasers in Engineering, 33(1), pp. 49-64.